Phase and Interface Control

Deutsche Ausgabe: DOI: 10.1002/ange.201606290
Internationale Ausgabe: DOI: 10.1002/anie.201606290

Phase and Interface Engineering of Platinum–Nickel Nanowires for Efficient Electrochemical Hydrogen Evolution

*Pengtang Wang, Kezhu Jiang, Gongming Wang, Jianlin Yao, and Xiaoqing Huang**

Abstract: *The design of high-performance electrocatalysts for the alkaline hydrogen evolution reaction (HER) is highly desirable for the development of alkaline water electrolysis. Phase- and interface-engineered platinum–nickel nanowires (Pt-Ni NWs) are highly efficient electrocatalysts for alkaline HER. The phase and interface engineering is achieved by simply annealing the pristine Pt-Ni NWs under a controlled atmosphere. Impressively, the newly generated nanomaterials exhibit superior activity for the alkaline HER, outperforming the pristine Pt-Ni NWs and commercial Pt/C, and also represent the best alkaline HER catalysts to date. The enhanced HER activities are attributed to the superior phase and interface structures in the engineered Pt-Ni NWs.*

Efficient hydrogen (H_2) production from water could potentially lead to a clean and renewable energy system.[1,2] Electrochemical water splitting to produce H_2 offers a reliable and sustainable solution for this purpose.[3,4] The catalysts are important components of water electrolysis cells and largely govern their performance.[5,6] To date, noble metals, such as Pt-based catalysts, are the most effective catalysts for HER with desirable performance, specifically in acidic electrolytes.[7,8] Despite excellent performance having been achieved on Pt-based catalysts in acidic water electrolysis, recently alkaline electrolysis is receiving extensive attention owing to its advantages, such as broad reactant availability and high product purity.[9] Unfortunately, the HER performance of Pt-based catalysts in alkaline electrolysis so far are not as good as that in acidic conditions,[10] which leads to high overpotential associated with large energy consumption for alkaline electrolysis.[11,12]

One strategy that has been used to address this tremendous challenge is integrating Pt nanostructures with the metal hydroxides,[13–16] since the edges of the metal hydroxides can promote the dissociation of water and the production of hydrogen intermediates, which subsequently adsorb on the nearby Pt surfaces and finally recombine into molecular hydrogen. This type of hybrid materials have exhibited much enhanced HER activity in basic conditions,[13–15] indicating that the sluggish kinetics of HER can be addressed via rationally constructing hybrid materials and fully exploiting the synergetic interactions between Pt and metal hydroxides.[13,17] In the past years, researchers have created various hybrid systems,[15,18] such as growth of noble metal NPs on the layered metal hydroxide[15] with improved water electrolysis kinetics in alkaline system. Despite these advances, the alkaline HER catalytic activities is still far from satisfactory.[19,20] At present, although some catalysts in alkaline condition can exhibit better HER activity than that of commercial Pt/C, the enhancement is only moderate.[15] The difficulty lies in the fact that the lattice spacing of metal hydroxides is usually larger than that of Pt, making it unfavorable to form intimate interface between metal hydroxides and Pt, which hinders the enhancement of HER activity.[14] Another challenge of current catalysts for alkaline HER is the unsatisfied durability, which is presumably due to the limited capability to resist the detrimental corrosive alkaline conditions.[20]

Herein, we develop a phase- and interface-engineered Pt-Ni NWs/C electrocatalyst through a simple yet effective post-annealing treatment under controlled atmosphere, with unprecedented HER activity. The Pt_3Ni_3 NWs/C-air have exceptional HER performance that is much better than the commercial Pt/C in alkaline solutions. In particular, the Pt_3Ni_3 NWs/C-air delivers unprecedented low overpotential of 40 mV at current densities of 10 mA cm^{-2} in 1 M KOH, which is the best activity among all the available HER electrocatalysts. Moreover, under long time durability test, the Pt_3Ni_3 NWs/C-air can maintain its catalytic activity for at least 3 h with only small activity loss.

We prepared the composition-segregated Pt-Ni NWs in high yield by modifying a previous method.[21] The compositions of Pt-Ni NWs were readily tuned by controlling the amount of $Ni(acac)_2$ supplied. It was found that all the prepared Pt-Ni NWs with various compositions have high yields, as revealed by TEM (Supporting Information, Figure S1). The Pt/Ni atomic ratio is determined to be 41.4:58.6 for Pt_3Ni_4 NWs, 48.9:51.1 for Pt_3Ni_3 NWs, 59.1:40.9 for Pt_3Ni_2 NWs, and 75.5:24.5 for Pt_3Ni_1 NWs by scanning electron microscopy energy-dispersive X-ray spectroscopy (SEM-EDS; Supporting Information, Figure S2). The Pt-Ni NWs were further characterized by powder X-ray diffraction (PXRD; Supporting Information, Figure S3). It is revealed that while the PXRD patterns of the Pt-Ni NWs display distinct face-centered cubic (*fcc*) patterns, each peak has a shoulder peak in the higher degree, indicating the presence of composition segregation in the Pt-Ni NWs. Associated with higher content of Ni, the presence of shoulder peak in each peak become more distinct. The highly composition segre-

[*] P. Wang, K. Jiang, Prof. J. Yao, Prof. X. Huang
College of Chemistry, Chemical Engineering and Materials Science
Soochow University, Jiangsu 215123 (China)
E-mail: hxq006@suda.edu.cn
Prof. G. Wang
Department of Chemistry, School of Chemistry and Material Science
University of Science and Technology of China
Hefei, Anhui 230026 (China)

Supporting information for this article can be found under: http://dx.doi.org/10.1002/anie.201606290.

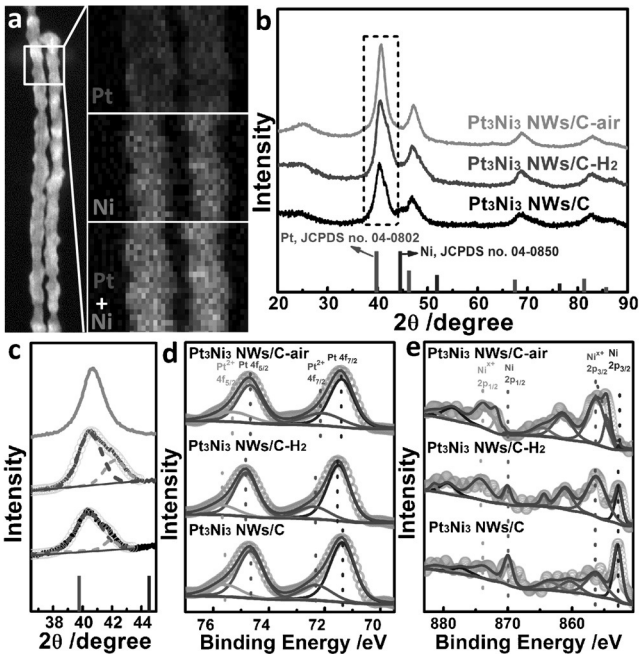

Figure 1. a) HAADF-STEM image and EDS elemental mappings of Pt_3Ni_3 NWs. b) PXRD patterns of Pt_3Ni_3 NWs/C, Pt_3Ni_3 NWs/C-H_2 and Pt_3Ni_3 NWs/C-air. c) The fitted peak curves from the dashed region marked in (b). XPS patterns of d) Pt 4f and e) Ni 2p of Pt_3Ni_3 NWs/C, Pt_3Ni_3 NWs/C-H_2 and Pt_3Ni_3 NWs/C-air.

gated feature was further characterized by the high-angle annular dark-field scanning transmission electron microscopy-EDS (HAADF-STEM-EDS) elemental mapping analysis (Figure 1 a), where the Pt is rich in the shell and Ni is concentrated in the inner region.

Considering that the highly composition-segregated metallic nanostructures are sensitive to the exposed atmosphere,[22] we turned our attention to the engineering of Pt-Ni NWs through thermal annealing at different atmospheres. To avoid aggregation during thermal annealing, we loaded the composition-segregated Pt_3Ni_3 NWs on C by mixing Pt_3Ni_3 NWs and C in cyclohexane, and then washed them with cyclohexane and ethanol. After mixing, the shape, composition, and the distribution of Pt_3Ni_3 NWs on C did not show obvious changes, as confirmed by the TEM and SEM-EDS (Supporting Information, Figure S4). The Pt_3Ni_3 NWs/C were then subjected to thermal annealing in the air at 250 °C for 1 h (termed as Pt_3Ni_3 NWs/C-air) and in the H_2/N_2 (5/95) at 300 °C (termed as Pt_3Ni_3 NWs/C-H_2), respectively. There are negligible composition changes of Pt_3Ni_3 NWs/C after thermal annealing in both air and H_2/N_2 (5/95), as characterized by SEM-EDS (Supporting Information, Figures S5, S6). To further analyze their structures, PXRD characterization for the Pt_3Ni_3 NWs/C, Pt_3Ni_3 NWs/C-air and Pt_3Ni_3 NWs/C-H_2 was carried out (Figure 1 b). While the PXRD pattern of Pt_3Ni_3 NWs/C-H_2 is almost the same with that of the pristine Pt_3Ni_3 NWs/C, the PXRD pattern of Pt_3Ni_3 NWs/C-air is significantly different, which displays the distinct *fcc* pattern precisely matching with the Pt_3Ni.[23] To carefully analyze the PXRD results, we enlarged the PXRD patterns between 36.5° to 43.5° (Figure 1 c). The peak of Pt_3Ni_3 NWs/C-air is symmetrical without shoulder peak, which can be indexed to the Pt_3Ni phase. On the contrast, the peaks of Pt_3Ni_3 NWs/C and Pt_3Ni_3 NWs/C-H_2 have shoulder peaks and can be separated into low-degree and high-degree peaks, which indicates the existence of Pt_3Ni and PtNi phase, respectively, as calculated by Vegard's law.[24] In addition to the phase, we further studied the chemical states of different nanomaterials by X-ray photoelectron spectroscopy (XPS). As shown in Figure 1 d, the Pt and Ni in the pristine Pt_3Ni_3 NWs/C have both metallic and oxidized states with the ratio of 2.81/1 for Pt^0/Pt^{2+} and 1/1.05 for Ni^0/Ni^{x+}. After being annealed in H_2/N_2 (5/95), the ratio of Pt^0/Pt^{2+} in Pt_3Ni_3 NWs/C-H_2 increases to 3.08/1 associated with the ratio of Ni^0/Ni^{x+} decreases to 1/3.09, which can be due to the reducibility of H_2 accelerating the electron transfer between Pt species and Ni species.[25] On the other hand, the ratio of Pt^0/Pt^{2+} after annealing in air decreases to 2.55/1 and the metallic Ni almost disappears, suggesting that the majority of Ni in the surface is oxidized.

The Pt_3Ni_3 NWs/C-air and Pt_3Ni_3 NWs/C-H_2 were further characterized by TEM and HAADF-STEM (Supporting Information, Figures S5, S6). Figure 2 a,b shows the HAADF-STEM images of the Pt_3Ni_3 NWs/C-air and Pt_3Ni_3 NWs/C-H_2, respectively. It clearly shows that the Pt_3Ni_3 NWs/C-air shows bright in the interior core associated with dark in their external surface, which is different from the pristine Pt_3Ni_3 NWs. The dark external surface of the Pt_3Ni_3 NWs/C-air with gaps suggests that the segregated-Ni in Pt_3Ni_3 NWs/C diffuses outwards and results in a filmy NiO_x shells after annealing in air.[26] As a contrast, any obvious changes cannot be observed for the Pt_3Ni_3 NWs/C-H_2, as compared with the pristine Pt_3Ni_3 NWs. As shown in Figure 2 c, Ni is rich in the

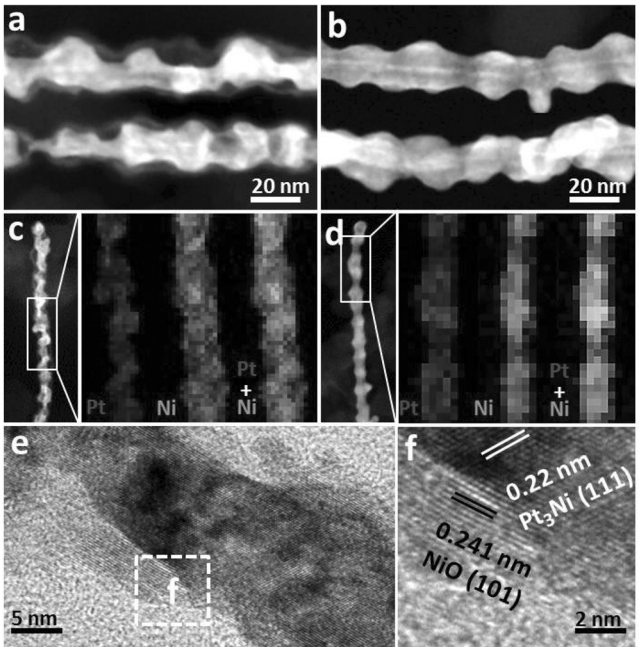

Figure 2. HAADF-STEM images of a) Pt_3Ni_3 NWs/C-air and b) Pt_3Ni_3 NWs/C-H_2. HAADF-STEM image and EDS elemental mappings of c) Pt_3Ni_3 NWs/C-air and d) Pt_3Ni_3 NWs/C-H_2. e) HRTEM image of Pt_3Ni_3 NWs/C-air and f) the magnified HRTEM image recorded from regions f marked in (e).

outer surface and Pt is concentrated in the interior core after the annealing treatment in air, which is dramatically different from the pristine Pt_3Ni_3 NWs. As indicated in Figure 2d, the elemental mapping shows that the Pt_3Ni_3 NWs/C-H_2 still exhibit Pt-rich shell structure, which is similar to that of the pristine Pt_3Ni_3 NWs. The HRTEM image clearly shows that the NiO_x shell with obvious gaps could not cover the Pt_3Ni-core completely (Figure 2e), which creates the exposed interfaces between NiO_x shell and Pt_3Ni core. The HRTEM image (Figure 2f) clearly displays the lattice fringes with interplanar spacing are 0.22 nm and 0.24 nm, which correspond to the (111) plane of Pt_3Ni and (101) plane of NiO, respectively. After simple thermal annealing treatment in the air, the phase and interface engineering have been achieved to transform the Pt_3Ni_3 NWs into unique NiO_x/Pt_3Ni heterostructures.

The annealing treatment at controlled atmospheres was also applied to Pt-Ni NWs/C with other compositions. Similar to that of Pt_3Ni_3 NWs/C, the Pt-Ni NWs with other compositions were loaded on the C (Supporting Information, Figure S7), and thermal annealed in air and H_2/N_2 (5:95), respectively. Since Pt_3Ni_1 NWs is a stable alloyed structure,[27] the TEM images, SEM-EDS and PXRD patterns of Pt_3Ni_1 NWs/C-air and Pt_3Ni_1 NWs/C-H_2 are similar to each other (Supporting Information, Figure S8). However, both the Pt_3Ni_2 NWs/C-air and Pt_3Ni_4 NWs/C-air display Pt_3Ni-core NiO_x-shell structures, as confirmed by TEM and elemental mappings (Supporting Information, Figures S9a,c, S10a). Meanwhile, the shoulder peaks in PXRD of Pt_3Ni_2 NWs/C-air and Pt_3Ni_4 NWs/C-air have been vanished after thermal annealing in air (Supporting Information, Figures S9e, S10d). With the Ni content in Pt-Ni NWs/C-air increasing, the NiO_x shell becomes denser and denser, which indicates the density of NiO_x/Pt_3Ni interfaces can be readily controlled.

To study the effect of the engineered interface and phase on HER catalysis of the Pt_3Ni_3 NWs/C-air, the HER electrocatalytic activity of the Pt_3Ni_3 NWs/C-air was thoroughly evaluated in both alkaline and acidic solution at scan rate of 10 mV s^{-1} and room temperature (Figure 3). Figure 3a,b shows the HER polarization curves of four different catalysts in 0.5 M and 0.05 M H_2SO_4, respectively. In general, all of the catalysts have similar activities in 0.5 M and 0.05 M H_2SO_4. In contrast, all PtNi NWs/C displays higher HER activities than commercial Pt/C in 0.1 M and 1 M KOH (Figure 3d,e). More significantly, in the higher alkaline solution (1 M KOH), the HER activity of Pt_3Ni_3 NWs/C-air is largely enhanced, representing the maximum performance (Figure 3e). To quantitatively compare the activities of these four catalysts, the current densities at −0.07 V versus RHE in 0.05 M&0.5 M H_2SO_4 and 0.1 M and 1 M KOH are summarized in Figure 3c and Figure 3f, respectively. It is clear that the activity of Pt_3Ni_3 NWs/C-air is humble in acidic solution but very promising in alkaline condition, particularly in the 1 M KOH. For example, the current density of Pt_3Ni_3 NWs/C-air at −0.07 V in 0.5 M H_2SO_4 is almost the same as that of the Pt/C, while the current density of Pt_3Ni_3 NWs/C-air at −0.07 V in 1 M KOH is 19.8 mA cm^{-2}, which is 6 times higher than that of the Pt/C (3.3 mA cm^{-2}). Unexpectedly, the activity of Pt_3Ni_3/C-air in 1 M KOH is much higher than that of in 0.1 M KOH, which is contrary to Pt/C. It is generally accepted that the HER catalysis has strong dependence on pH and low pH is beneficial for HER catalysis,[28] however it was not observed on the Pt-Ni/C-air.

Besides pH effects, we also studied the composition dependent HER activities in alkaline condition. Figure 4a shows the HER activity of Pt-Ni NWs/C-air with different compositions in 1 M KOH without IR compensation. It is clear that the HER activity of these four catalysts follows the sequence as: Pt_3Ni_3 NWs/C-air > Pt_3Ni_2 NWs/C-air > Pt_3Ni_1 NWs/C-air > Pt_3Ni_4 NWs/C-air. The activity of Pt_3Ni_4 NWs/C-air has a large disparity compared with others, which illustrates that the HER activity could not be promoted by solely increasing the content of Ni. The HER activities in 0.1 M KOH also exhibit similar trend as that of in 1 M KOH (Figure 4b). However, the activity differences among the Pt-Ni NWs/C-air in 0.1 M KOH are smaller than those of in 1 M KOH. Moreover, the activities of Pt-Ni NWs/C-air in 1 M KOH are generally higher than their corresponding activities in 0.1 M KOH. To compare the HER activity of Pt-Ni NWs/C-

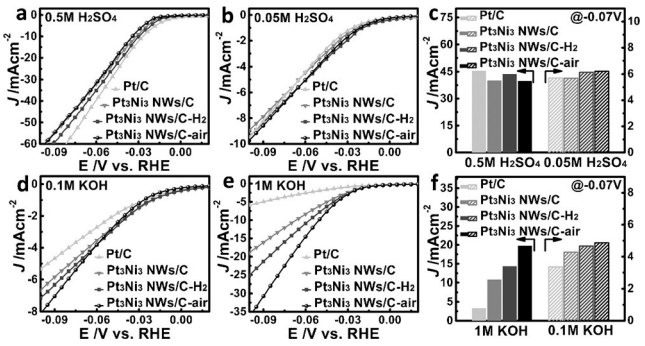

Figure 3. HER activities of different electrocatalysts in a) 0.5 M H_2SO_4, b) 0.05 M H_2SO_4, d) 0.1 M KOH and e) 1 M KOH. Histograms of activities at −0.07 V versus RHE from c) Figure 4a,b and f) Figure 4d,e. Geometric area of RDE is 0.196 cm^2.

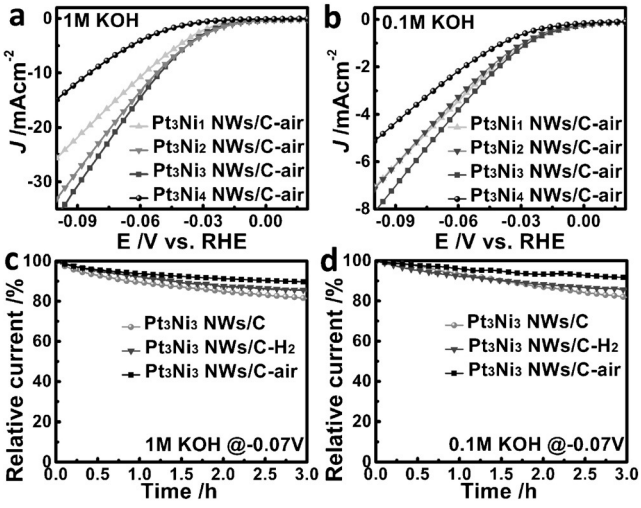

Figure 4. HER activities of different electrocatalysts in a) 1 M KOH and b) 0.1 M KOH at room temperature. Normalized chronoamperometric curves of different electrocatalysts under a constant potential of −0.07 V versus RHE in c) 1 M KOH and d) 0.1 M KOH.

air with previously reported electrocatalysts, we also tested the HER performance with IR compensation in alkaline media (Supporting Information, Figure S11). Pt_3Ni_3 NWs/C-air exhibit the highest activity of 39.7 and 23.0 mA cm^{-2} at −0.07 V in 1M and 0.1M KOH, respectively, which is 11.6 times and 2.8 times higher than that of the commercial Pt/C (3.42 mA cm^{-2} in 1M KOH and 8.1 mA cm^{-2} in 0.1M KOH). To our best knowledge, by comparing the current densities at −0.07 V versus RHE and overpotentials at 10 mA cm^{-2}, the Pt_3Ni_3 NWs/C-air outperform all the reported electrocatalysts (Supporting Information, Table S1).

Durability is another important parameter to evaluate the performance of HER catalysts; the stability of Pt-Ni NWs/C-air was thus evaluated by using chronoamperometry. Figure 4c shows the normalized chronoamperometric curves at the potential of −0.07 V in 1M KOH. It reveals that Pt_3Ni_3 NWs/C-air maintain 90.1% of its initial activity in 1M KOH after 3 h test, while Pt_3Ni_3 NWs/C-H_2 and Pt_3Ni_3 NWs/C keep 85.5% and 81.3% of their initial activity, respectively, indicating an enhanced stability of Pt_3Ni_3 NWs/C-air in 1M KOH. Similar stability trend was also observed in 0.1M KOH, where the Pt_3Ni_3 NWs/C-air also displays the best stability with 91.7% activity maintained after 3 h, compared with 85.8% of Pt_3Ni_3 NWs/C-H_2 and 81.8% of Pt_3Ni_3 NWs/C (Figure 4d). Such enhanced stability of Pt_3Ni_3 NWs/C-air can be also confirmed by chronopotentiometry test (Supporting Information, Figure S12). Therefore, the presence of proper NiO_x/Pt_3Ni interfaces in Pt-Ni NWs/C-air can not only boost the HER activity but also enhance the HER stability in alkaline media (Supporting Information, Figure S13).

In general, the pathways of the HER in alkaline media can be typically classified as Volmer–Tafel pathway and Volmer–Heyrovsky pathway.[13] In the first step, the Volmer step involves the water dissociation and formation of the intermediate H_{ads}. The intermediate H_{ads} need a suitable driving force and site to be absorbed and then generate H_2. Although Pt has been calculated to have the optimal H atom binding energy so far, it is poor at cleaving the HO–H bond to dissociate the water in the first step. Moreover, the OH^- generated by H_2O splitting in Volmer step will also block the active catalytic sites of Pt and thus influence the second step. On the NiO_x/Pt_3Ni interface, the NiO_x can accelerate the water dissociation and it has a stronger electrostatic affinity with OH^- than Pt due to the unfilled d-orbitals of Ni^{x+}. Thus, while the OH^- produced by H_2O splitting will adhere on NiO_x site at the interface, a nearby vacant Pt site would adsorb H_{ads} readily to produce H_2. Such synergistic effect at the NiO_x/Pt_3Ni interface enhances the HER performance in alkaline media eventually.

To further understand the synergistic effect of NiO_x/Pt_3Ni interfaces on the HER performance of our catalysts, an illustration of the interface and phase engineering of Pt-Ni NWs/C is shown in Figure 5. It is clearly shown that the Pt-Ni NWs/C-H_2 have minimum phase and structure changes and limited NiO_x/Pt_3Ni interface after annealing in the H_2/N_2 (5:95). In sharp contrast, after thermal annealing in air the Pt-Ni NWs/C with different compositions not only undergoes the phase changes but also shows high density of NiO_x/Pt_3Ni interfaces. As shown in Figure 5b, although the formation of

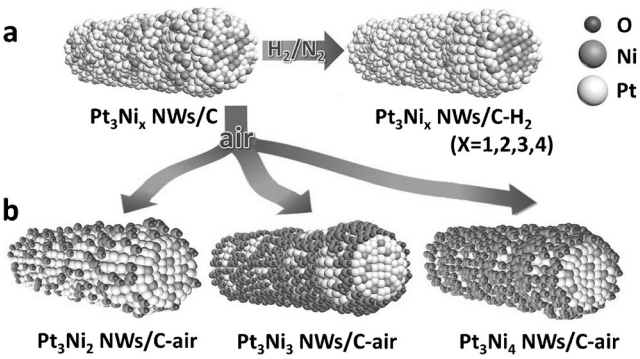

Figure 5. a) The changes of Pt-Ni NWs/C-H_2 by annealing the Pt-Ni NWs/C in H_2/N_2(5/95). b) The changes of Pt_3Ni_2 NWs/C-air, Pt_3Ni_3 NWs/C-air, and Pt_3Ni_4 NWs/C-air by annealing the Pt-Ni NWs/C in air.

NiO_x/Pt_3Ni interfaces is observed in the Pt_3Ni_2 NWs/C-air, there are limited NiO_x/Pt_3Ni interfaces on the surface of the Pt_3Ni_2 NWs/C-air owing to the insufficient amounts of NiO_x, which may not able to absorb the OH^- efficiently, resulting in limited enhancement of HER. With the increase of Ni in Pt-Ni NWs/C-air (that is, Pt_3Ni_3 NWs/C-air), the NiO_x shell becomes denser, which will provide more sites to absorb the OH^- in time and therefore enhance the HER performance. However, If the NiO_x-shell becomes too dense (that is, Pt_3Ni_4 NWs/C-air), the Pt_3Ni-core would be coated too intact to expose enough NiO_x/Pt_3Ni interfaces to electrolyte, which results in moderate HER performance (Supporting Information, Figure S14). Hence, proper composition with optimized interfaces of NiO_x/Pt_3Ni are critical to the HER performance.

In summary, we have successfully created a new class of Pt-Ni NWs/C-air with engineered interfaces and phases by simple thermal annealing of the highly composition-segregated Pt-Ni NWs/C in air. Benefitting from the unique 1D structure, controlled interfaces and phases between the Pt_3Ni and NiO_x, the Pt-Ni NWs/C-air exhibits promising activity for alkaline HER. Particularly, the Pt_3Ni_3 NWs/C-air exhibits the highest HER activity among all the Pt-Ni NWs/C-air in 1M KOH solution. These Pt-Ni NWs/C-air catalysts also exhibit enhanced durability with limited decay after long-term chronoamperometry test. This study provides a new surface and phase-engineering strategy for designing unique catalysts with excellent electrocatalytic performance for HER and beyond.

Acknowledgements

This work was financially supported by the start-up funding from Soochow University, Young Thousand Talented Program, the National Natural Science Foundation of China (21571135), and the Priority Academic Program Development of Jiangsu Higher Education Institutions (PAPD).

Keywords: hydrogen evolution reaction · nanowires · nickel · phase and interface control · platinum

How to cite: *Angew. Chem. Int. Ed.* **2016**, *55*, 12859 – 12863
Angew. Chem. **2016**, *128*, 13051 – 13055

[1] M. G. Walter, E. L. Warren, J. R. McKone, S. W. Boettcher, Q. Mi, E. A. Santori, N. S. Lewis, *Chem. Rev.* **2010**, *110*, 6446 – 6473.
[2] M. Dresselhaus, I. Thomas, *Nature* **2001**, *414*, 332 – 337.
[3] S. Gu, B. Xu, Y. Yan, *Annu. Rev. Chem. Biomol. Eng.* **2014**, *5*, 429 – 454.
[4] J. A. Turner, *Science* **2004**, *305*, 972 – 974.
[5] C. G. Morales-Guio, L.-A. Stern, X. Hu, *Chem. Soc. Rev.* **2014**, *43*, 6555 – 6569.
[6] T. J. Meyer, *Nature* **2008**, *451*, 778 – 779.
[7] J. K. Norskov, C. H. Christensen, *Science* **2006**, *312*, 1322 – 1323.
[8] S. Bai, C. Wang, M. Deng, M. Gong, Y. Bai, J. Jiang, Y. Xiong, *Angew. Chem. Int. Ed.* **2014**, *53*, 12120 – 12124; *Angew. Chem.* **2014**, *126*, 12316 – 12320.
[9] K. Zeng, D. Zhang, *Prog. Energy Combust. Sci.* **2010**, *36*, 307 – 326.
[10] P. Rheinländer, S. Henning, J. Herranz, H. A. Gasteiger, *ECS Trans.* **2013**, *50*, 2163 – 2174.
[11] L. M. Gandía, R. Oroz, A. Ursúa, P. Sanchis, P. M. Diéguez, *Energy Fuels* **2007**, *21*, 1699 – 1706.
[12] M. Janjua, R. Le Roy, *Int. J. Hydrogen Energy* **1985**, *10*, 11 – 19.
[13] R. Subbaraman, D. Tripkovic, D. Strmcnik, K.-C. Chang, M. Uchimura, A. P. Paulikas, V. Stamenkovic, N. M. Markovic, *Science* **2011**, *334*, 1256 – 1260.
[14] N. Danilovic, R. Subbaraman, D. Strmcnik, K. C. Chang, A. Paulikas, V. Stamenkovic, N. M. Markovic, *Angew. Chem. Int. Ed.* **2012**, *51*, 12495 – 12498; *Angew. Chem.* **2012**, *124*, 12663 – 12666.
[15] H. Yin, S. Zhao, K. Zhao, A. Muqsit, H. Tang, L. Chang, H. Zhao, Y. Gao, Z. Tang, *Nat. Commun.* **2015**, *6*, 6430.
[16] W. Huang, H. Wang, J. Zhou, J. Wang, P. N. Duchesne, D. Muir, P. Zhang, N. Han, F. Zhao, M. Zeng, *Nat. Commun.* **2015**, *6*, 10035.
[17] R. Subbaraman, D. Tripkovic, K.-C. Chang, D. Strmcnik, A. P. Paulikas, P. Hirunsit, M. Chan, J. Greeley, V. Stamenkovic, N. M. Markovic, *Nat. Mater.* **2012**, *11*, 550 – 557.
[18] H. Fei, J. Dong, M. J. Arellano-Jiménez, G. Ye, N. D. Kim, E. L. Samuel, Z. Peng, Z. Zhu, F. Qin, J. Bao, *Nat. Commun.* **2015**, *6*, 8668.
[19] Z. Weng, W. Liu, L.-C. Yin, R. Fang, M. Li, E. I. Altman, Q. Fan, F. Li, H.-M. Cheng, H. Wang, *Nano Lett.* **2015**, *15*, 7704 – 7710.
[20] M. Gong, W. Zhou, M.-C. Tsai, J. Zhou, M. Guan, M.-C. Lin, B. Zhang, Y. Hu, D.-Y. Wang, J. Yang, *Nat. Commun.* **2014**, *5*, 4695.
[21] L. Bu, J. Ding, S. Guo, X. Zhang, D. Su, X. Zhu, J. Yao, J. Guo, G. Lu, X. Huang, *Adv. Mater.* **2015**, *27*, 7204 – 7212.
[22] M. Ahmadi, F. Behafarid, C. Cui, P. Strasser, B. R. Cuenya, *ACS Nano* **2013**, *7*, 9195 – 9204.
[23] X. Huang, E. Zhu, Y. Chen, Y. Li, C. Y. Chiu, Y. Xu, Z. Lin, X. Duan, Y. Huang, *Adv. Mater.* **2013**, *25*, 2974 – 2979.
[24] A. R. Denton, N. W. Ashcroft, *Phys. Rev. A* **1991**, *43*, 3161.
[25] K. Jiang, P. Wang, S. Guo, X. Zhang, X. Shen, G. Lu, D. Su, X. Huang, *Angew. Chem. Int. Ed.* **2016**, *55*, 9030 – 9035; *Angew. Chem.* **2016**, *128*, 9176 – 9181.
[26] S. Liu, Q. Zhang, Y. Li, M. Han, L. Gu, C. Nan, J. Bao, Z. Dai, *J. Am. Chem. Soc.* **2015**, *137*, 2820 – 2823.
[27] J. Zhang, J. Fang, *J. Am. Chem. Soc.* **2009**, *131*, 18543 – 18547.
[28] W. Sheng, Z. Zhuang, M. Gao, J. Zheng, J. G. Chen, Y. Yan, *Nat. Commun.* **2015**, *6*, 5848.

Received: June 28, 2016
Revised: July 29, 2016
Published online: September 15, 2016

